RESEARCH ARTICLE VOLCANICA

The influence of regional stress and structural control on the shape of maar craters

Cody Nichols*, Alison Graettinger
Department of Earth and Environmental Sciences, University of Missouri-Kansas City. Kansas City MO, 64110, USA.

Abstract

Maars are volcanic craters surrounded by ejecta rings. The craters are excavated by subsurface explosions, commonly attributed to the interaction of magma and groundwater in phreatomagmatic explosions. Maar craters have a variety of shapes and sizes, but commonly are elongate. This paper explores the relationship between the orientation of maar elongation and regional stress indicators. The orientations of maar elongation, regional faults, and nearest neighbor lineaments containing maars were measured in seven volcanic fields: Auckland (New Zealand), Lamongan (Indonesia), Newer Volcanics Province (Australia), Pali Aike (Argentina), Pinacate (Mexico), Macolod Corridor (Philippines), and Serdán Orientale (Mexico). Common maar orientations were observed in several fields and compared with faulting and nearest neighbor lineaments. It was found that the *distribution* of maars was commonly correlated with regional stress indicators including regional faults and lineaments of aligned vents, but the *orientation of elongation* of those maars did not always correlate with stress indicators. Maars not aligned with stress indicators were likely influenced by more local effects, including changes to the subsurface stress regime from the ongoing eruption.

Keywords: `Phreatomagmatic; Orientation; Propagation; Distribution; Stress regime; Elongation`

1 Introduction

Maars are volcanic landforms produced by subsurface phreatomagmatic explosions that result in a distinctive crater with a floor beneath the pre-eruptive surface, and a surrounding ejecta ring. Maar craters are the product of tens to hundreds of discrete explosions attributed to contact between magma and groundwater [Ross et al. 2017; Valentine et al. 2017; White and Ross 2011]. These subsurface explosions produce an inverted cone of debris in the subsurface (the diatreme), with the crater and tephra ring the only surface expression (Figure 1). Although these eruptions generate craters of varying size and shape, the majority of maars exhibit elongate to complex shapes [Graettinger 2018]. Unlike scoria cones, maars are not constructional landforms, instead the shape of maar craters is controlled by explosive excavation and collapse [White and Ross 2011, and references therein]. Although maars can frequently be found in spatial association with scoria cones, the process of excavation by subsurface explosions warrants separate evaluation from scoria cone construction. It is therefore important to evaluate populations of maars, across multiple volcanic fields, to assess external influences on crater growth to inform hazard models regarding their formation and subsequent propagation in the field.

More than half of the world's maars occur in monogenetic volcanic fields alongside scoria cones and other small vents, but 42 % occur within complex volcanic fields next to (maars in the Macolod Corridor Philippines) and as parasitic features on larger structures like stratovolcanoes (Lamongan Volcanic Field, Indonesia) and calderas (Aniakchak, USA) [Graettinger 2018]. The distribution and alignment of small volume volcanic edifices, such as scoria cones, has been used to recognize the distribution and orientation of magma pathways in the crust, including fractures produced by the arriving magma and the exploitation of pre-existing fractures [Cebriá et al. 2011; Corazzato and Tibaldi 2006; Germa et al. 2013; Hernando et al. 2014; López Loera et al. 2008; Mazzarini 2003; Tibaldi 1995]. Similar studies of calderas in the Ethiopian rift have also identified an elongation of the caldera shape paralleling pre-rift fractures reflecting tectonic influences even on much larger structures [Acocella et al. 2003; Robertson et al. 2015]. The influence of regional stress and structural control has been observed in multiple tectonic settings [Le Corvec et al. 2013a], but local influences on individual cones and clusters can also be detected across large volcanic fields [Connor et al. 1992; Maccaferri et al. 2015].

This study aims to evaluate the influence of regional stress on the distribution and shapes of maar volcanoes across seven volcanic fields in different tectonic settings. Indicators of regional stress, including regional faults and lineaments of aligned vents were compared

*Corresponding author: Nichols.c@outlook.com

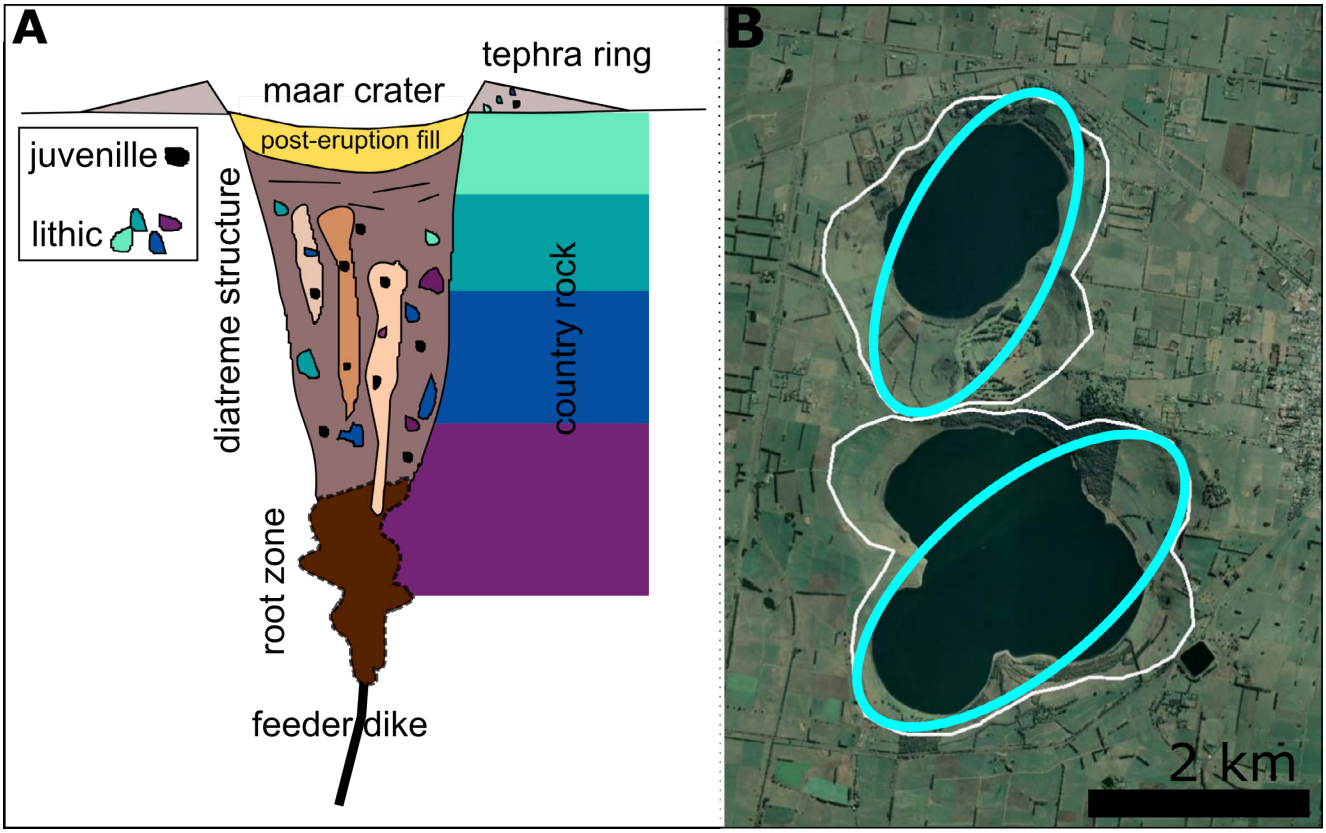

Figure 1: [A] Cartoon showing the idealized subsurface structure of a maar crater with colors representing the mixing inside the diatreme of volcanic and country rock materials. [B] Gnotuk (top) and Bullen Merri (bottom) maars (Newer Volcanic Province, Australia) with polygon of crater outline with ellipse for elongation superimposed. Note that Bullen Merri has two measurable directions of elongation.

with the orientation of the primary direction of elongation of well-preserved maars within the Auckland Volcanic Field (New Zealand), Lamongan Volcanic Field (Indonesia), Newer Volcanics Province (Australia), Pali Aike Volcanic Field (Argentina), Pinacate Volcanic Field (Mexico), maars of the Macolod Corridor (Philippines), and Serdán Oriental Volcanic Fields (Mexico; Figure 2). These fields were selected as they had large numbers (>5) of intact maars and represented a range of volcanic and tectonic environments. This is the first effort to evaluate the influence of the regional stress regime on the growth of maars across multiple volcanic fields.

1.1 Auckland Volcanic Field

The Auckland Volcanic Field (AVF) on the North Island of New Zealand is an intraplate monogenetic field located roughly 400 km west of the present-day Hikurangi subduction zone [Cassidy and Locke 2010; Hopkins et al. 2020]. The field occupies an area of 336 km^2 and contains more than 53 small monogenetic volcanic centers, many of which are phreatomagmatic including the six maars used in this study [Kereszturi et al. 2014]. The field has been active from <250 ka to 500 years before present [Lindsay et al. 2011], producing predominately alkali basalts and basanites and erupting through Miocene-Eocene age alternating sequences of sandstones and mudstones that rest on top of Mesozoic metasedimentary terranes [Mortimer et al. 2014]. Miocene-Quaternary extensional block faulting produced faults striking NNW and ENE throughout the region [Cassidy and Locke 2010; Kenny et al. 2012; Langridge et al. 2016].

1.2 Lamongan Volcanic Field

The Lamongan Volcanic Field (LVF) is located in east Java, Indonesia within the Sunda Volcanic Arc, a surface expression of the northward subduction of the Indo-Australian Plate beneath the Eurasian Plate [Carn 1999]. The 90 vents of the Lamongan volcanic field sit near and on the slopes of the Lamongan stratovolcano, covering an area of 260 km^2 and cutting through lacustrine sediments, lavas and pyroclastic deposits [Carn 1999; Carn 2000; Pirrung et al. 2004]. From these vents, fourteen maars were selected for use in this study. The field has been active for approximately 20,000 years, containing lava flows and cones that range in composition from basalt to basaltic andesite [Carn 1999; Pir-

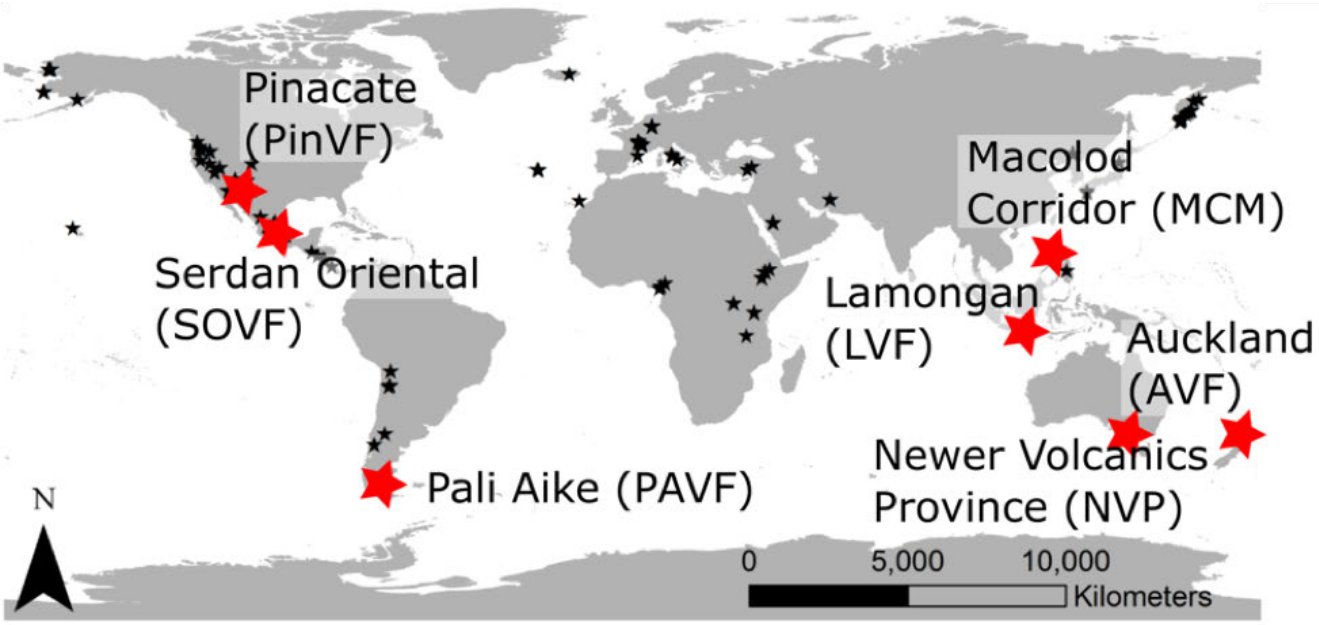

Figure 2: Location of volcanic fields (red stars) in this study overlain on the map of maars in the MaarVLS database (black stars; Graettinger [2018]).

rung et al. 2004]. The tectonic structure beneath the field is poorly understood, however radar imagery provides some evidence for regional NW–SE and NE–SW faulting [Carn 1999].

1.3 Newer Volcanics Province

The Newer Volcanics Province (NVP) is an intraplate monogenetic volcanic region located in southeastern Australia. The area covers more than 19,000 km^2 and contains over 400 eruptive vents [Boyce 2013], including the 23 maars included in this study. Most of the maars of the NVP (and all of the maars utilized in this study) fall within the Otway Basin, an extensional basin formed during the break-up of Australia and east Antarctica at the end of the Jurassic [Kharazizadeh et al. 2017]. Eruptive products in the NVP range from tholeiitic to alkali basalt dated from the Pliocene through the Holocene [Lesti et al. 2008]. The majority of the maars occur in the southern part of the NVP. All of the maars used cut through the Cretaceous-Pliocene sedimentary sequence of the Otway Basin and lavas from earlier activity in the NVP [Boyce 2013; Jordan et al. 2013; Kharazizadeh et al. 2017; Lesti et al. 2008]. This sedimentary sequence is deposited directly on top of the Paleozoic basement [Lesti et al. 2008]. The region is crosscut by multiple major fault lines, predominately oriented in a North-South direction.

1.4 Pali Aike Volcanic Field

The Pali Aike Volcanic Field (PAVF) marks a major Pliocene–Quaternary phase in the development of the Magellan Neogene rift system in Southern Argentina and Chile [D'Orazio et al. 2000; Mazzarini 2003]. The 4500 km^2 field contains 476 eruptive features including numerous maars, of which 23 of the best preserved were analyzed here. Activity in the PAVF has been dated from 3.78 to 0.17 Ma, although young fresh morphology lava flows suggest continued activity into the Holocene [Mazzarini 2003]. The PAVF deposits are predominantly alkaline basalts and basanites [D'Orazio et al. 2000; Ross et al. 2011]. The field is built on top of volcano-sedimentary infill with a Paleozoic metamorphic basement [Mazzarini 2003]. Maars cut through these sequences and earlier lavas of PAVF activity [Haller and Németh 2006; Ross et al. 2011]. Faults and lineaments in the region have dominant ENE–WSW and NW–SE orientations [Mazzarini 2003].

1.5 Pinacate Volcanic Field

The Pinacate Volcanic Field (PinVF) of Sonora, Mexico, lies just a few kilometers east of the Gulf of California within the Gulf Extensional Province [García-Abdeslem and Calmus 2015; Gutmann 2002]. Over 400 vents, including eight maars studied here, formed within the Late Pleistocene 1500 km^2 monogenetic PinVF, with numerous morphologically young features present [García-Abdeslem and Calmus 2015; Turrin et al. 2008]. Pinacate volcanics are alkaline to transitional basalts with rare tholeiites [Turrin et al. 2008]. Pinacate maars cut through the gravelly deposits of the ancestral Sonoyta River that sit on a sequence of thick basaltic lava flows and basin-filling sediment on top of a Miocene basaltic basement [García-Abdeslem and Calmus 2015; Gutmann 2002]. Nearby, the Pacific–

North American plate boundary is defined by the right lateral, NW–SE-trending, Imperial and Cerro Prieto faults [García-Abdeslem and Calmus 2015; Padilla et al. 2013].

1.6 Maars of the Macolod Corridor

Torn between Eastward subduction along the Manila Trench, and Westward subduction along the Philippine Trench, the Macolod Corridor is a zone of extensional faulting between the two [Vogel et al. 2006]. The space between these two segments of the Luzon Arc is about 80 km wide and trends NE [Vogel et al. 2006]. The Macolod Corridor likely intersects several different outcrops including Zambales type ophiolites, Central Valley clastics, and Angat Ophiolites moving from the Southwest to Northwest respectively [Defant et al. 1988]. Within the corridor are located hundreds of maars, a couple calderas, and three stratovolcanoes, though the maars chosen for this study are grouped near the center of the corridor and include the San Pablo City Volcanic Field [Ku et al. 2009]. The 16 maars chosen from the Macolod Corridor (MCM) are nestled between Mt Maquilung, Mt Crostbal/Mt Banahaw stratovolcanoes and Taal caldera. Activity in the Macolod Corridor dates from ~2 Ma, but more detailed age information is not available on the small volcanic features like maars in the area [Ku et al. 2009; LLDA 2014]. The lavas of the Macolod Corridor are almost exclusively basaltic [Förster et al. 1990], with the northeastern section hosting the MCM having more calc-alkaline basalt compositions [Ku et al. 2009]. The maars of this field cut through mixed volcanic deposits from the surrounding calderas and smaller volcanic centers. The MCM lies at the northeastern edge of the Macolod Corridor surrounded by N-S and E-W trending fault systems [Förster et al. 1990; Tsutsumi and Perez 2013] with common NE–SW normal faults crosscutting larger volcanic edifices [Irapta 2018].

1.7 Serdán Orientale Volcanic Field

The Serdán-Oriental Volcanic Field (SOVF) lies in the easternmost part of the Trans Mexican Volcanic Belt, in a broad, internally drained intermountane basin [Carrasco-Núñez et al. 2007]. Covering approximately 5250 km^2, the SOVF contains tens of vents including rhyolitic domes, scoria cones, lavas, maars, tuff rings, and a few tuff cones [Carrasco-Núñez et al. 2007; Ort and Carrasco-Núñez 2009]. Nine maars from the SOVF were included in this study. Volcanism in the Serdán Oriental basin has been active since the Pliocene epoch, but the maars are predominantly late Pleistocene in age [Carrasco-Núñez et al. 2007]. The SOVF is the only field in this study that contains rhyolitic and basaltic maars. The maars cut pyroclastic deposits, Pleistocene basaltic lava flows, and the underlying limestone basement [Carrasco-Núñez et al. 2007]. Intra-arc active extensional-faulting in the central part of the Mexican Volcanic Belt follows a general E–W or ENE–WSW trend with the least horizontal stress oriented in the N-S direction [Carrasco-Núñez et al. 2007; Ferrari et al. 2000; Padilla et al. 2013; Suter et al. 1992].

2 Methods

In order for a maar to be eligible for inclusion in elongation orientation analysis, it had to have a visually discernable and complete crater rim. The rims of selected maars were manually digitized using imagery available in Google Earth. Using the ellipse tool in Arc GIS, an ellipse was then fit within the maar rim polygon such that it occupied the largest possible area without crossing the boundaries of the polygon, to represent the primary direction of elongation of the crater (Figure 1). In cases where the largest area covered by an ellipse proved to be circular (aspect ratio of >0.9), the maar was removed from the dataset. Orientations of elongation determined this way are reasonable within ten degrees.

For this study, stress indicators include exposed regional faults and lineaments of aligned volcanic features. Regional faults were selected within and around the studied volcanic fields based on proximity, from published literature and government datasets of mapped faults and lineaments. The number of faults from some fields were limited likely due to significant cover by sediments and volcanic deposits. All fault lineaments within 50 km of the center of each field were digitized. In cases where faults were not well exposed or mapped, the range was extended to 150 km (AVF and PinVF). The azimuthal orientation of the faults was calculated and tabulated.

A maar-focused nearest neighbor analysis was carried out for all maars digitized (not just those used for elongation orientation) using the centroid of the original polygons to compute the orientation of the line between the two nearest neighbor maar craters. Lineations of aligned maars were identified where three or more maars were found in a line, and the orientation of that line fell within ten degrees of a nearest neighbor mode. Age of the landforms was not considered in this selection, however the fields used were selected for being quaternary in age. Where available, focused vent alignment studies from Le Corvec et al. [2013b], Mazzarini [2003], Pirrung et al. [2004], and Boyce [2013] were used to evaluate the success of maar-generated nearest neighbor alignment and to compare with maar orientation data. For the Lamongan volcanic field and the Macolod Corridor the position information on non-maar vents is limited in the literature and positions are difficult to discern with satellite imagery alone due to heavy vegetation cover, so similar comparison could not be drawn.

Angle	Number	Slope
-5	0	
1	1	6.5
8	2	4.5
10	3	2.5
13	4	7.5
25	5	22.5
58	6	28
81	7	16
90	8	5
91	9	3
96	10	8.5
108	11	13.5
123	12	8.5
125	13	6.5
136	14	7.5
140	15	3
142	16	2.5
145	17	3
148	18	6
157	19	9
166	20	6.5
170	21	3
172	22	2.5
175	23	4.5
181	24	

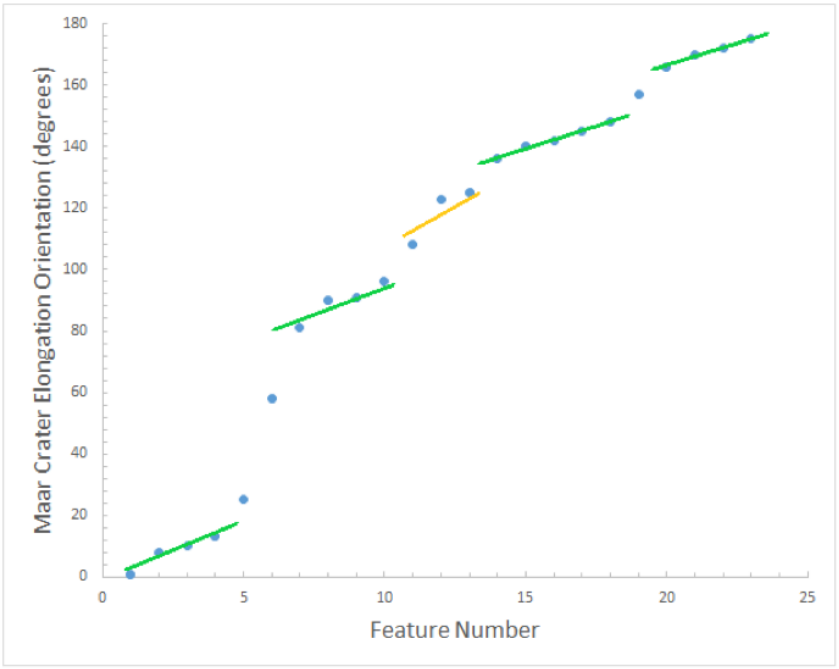

Figure 3: Graph of primary elongation orientations for maars in the Pali Aike Volcanic Field and line used to classify modes of shared orientations. Areas in which the slope is less than five are highlighted green, making up the strong modes. Areas of the line highlighted yellow have a slope less than ten and make up weak modes.

A mode represents frequently occurring values in a dataset, representing a common orientation. Orientation modes were determined for primary maar elongation, fault orientation, and nearest neighbor lineament orientation. Orientations were plotted in ten degree bins as rose diagrams for visual evaluation, but as modes in natural datasets can be influenced by the method of defining the mode (including binning), especially when datasets are small, an additional cluster determination was used to define strong and weak modes. Orientation measurements for a field were ordered from smallest to largest and plotted on a simple line plot. The slope of line varied between similar values (Figure 3). In most of the studied volcanic fields the datasets were small, due to the number of available maars, and a shallow slope, of five or less between orientation values, was used to identify 'strong' modes. When the slope of the line was up to ten the mode was considered 'weak'. Modes are assigned by a code of P = Primary elongation, F = fault orientation, and N = Nearest neighbor orientation with a subscript A–X to distinguish them (where A is the strongest). Because the amount of fault data for the Newer Volcanics Province was substantially larger than what was available for all other data sets (more than six times as many data points as other fields), modes were manually determined with the assistance of the slope method after lowering the required slope threshold to 2.5 and 5 for strong and weak modes respectively.

3 Results

3.1 Auckland Volcanic Field

AVF has a total of six maars with measurable elongation. The maars exhibit no strong or weak modes in primary elongation orientation (Figure 4; Table 1). The faulting data exhibit a single strong mode (F_A) from 154–168°. Maar-derived nearest neighbor direction data exhibits one strong mode from 19–25° (N_A) supported by a lineament of three or more aligned maars in field (Figure 4). Out of all the maars, only one elongation orientation falls within ten degrees of the faulting mode F_A. Nearest neighbor analysis that involved 49 volcanic vents (of any vent type) by Le Corvec et al. [2013b] revealed three lineaments composed of vents with two different orientations (NE–SW and NNE–SSW) consistent with Von Veh and Németh [2009]. The observed orientations of nearest neighbor maar pairs match with these larger trends in the field. The orientations of maar elongations were diverse in the AVF and no correlation between the elongation and stress indicators was apparent.

3.2 Lamongan Volcanic Field

Lamongan Volcanic Field contains fourteen maars with measurable orientations of elongation (Table 1). The maars of LVF exhibit one strong primary elongation ori-

Table 1: Summary of modes identified in this study and related literature.

Volcanic Field	Elongation modes		Faulting Modes		NN modes		Literature
Auckland	-	-	F_A	154-168°	N_A	19-25°	NE–SW*
	-	-	-	-	-	-	NNE–SSW*
Lamongan	P_A, $n = 5$	179–11°	F_A	68–78°	N_A	144–155°	-
	P_C, $n = 3$‡	24–41°	F_B	135–150°	-	-	-
Newer	P_A, $n = 10$	9–41°	F_A	78–123°	N_A	108–132°	90–120°**
	P_B, $n = 3$	167–176°	F_B	158–13°	N_B	139–139°	-
	P_C, $n = 5$‡	104–136°	F_C	123–140°	N_C‡	44–75°	30–60°**
	P_D, $n = 3$‡	46–63°	-	-	-	-	-
Pali Aike	P_A, $n = 5$	136–148°	F_A	119–146°	N_A	132–163°	NE–SW*
	P_B, $n = 4$	1–13°	F_B	48–51°	N_B	87–98°	-
	P_C, $n = 4$	81–96°	F_C	71–74°	N_C	98–110°	NW–SE*
	P_D, $n = 4$	166–175°	-	-	-	-	-
	P_E, $n = 3$‡	108–125°	-	-	-	-	-
Pinacate	P_A, $n = 3$	17–28°	F_A	127–153°	N_A	91–95°	NNW–SSE*
	-	-	-	-	-	-	NE–SW*
Macolod	P_A, $n = 3$	4–8°	F_A	27–68°	N_A	59–62°	-
	P_B, $n = 3$	31–40°	F_B	177–18°	N_B	153–161°	-
	P_C, $n = 3$	60–70°	F_C	90°	-	-	-
	P_D, $n = 3$‡	97–114°	-	-	-	-	-
Serdán O.	P_A, $n = 3$	70–77°	FA	118–154°	-	-	-
	-	-	FB	5–13°	-	-	-
	-	-	-	-	-	-	E–W†

* Le Corvec et al. [2013b]
** Boyce [2013]
† Suter et al. [1992] and De León-Barragán et al. [2020]
‡ weak mode

entation mode from 179–11° (P_A, $n = 5$), and one weak mode from 24-41° (P_C, $n = 3$; Figure 5). Faulting data from LVF exhibits two strong modes at 68–78° (F_A) and 135–150° (F_B). The maar derived nearest neighbor direction data in Lamongan has one strong mode from 144–155° (N_A) supported by three or more aligned maars. Nearest neighbor mode N_A falls entirely within ten degrees of the edges of faulting mode F_B. There is no overlap shared by either nearest neighbor or faulting data with maar elongation orientations for this field. Although comprehensive nearest neighbor analysis of the entire Lamongan Volcanic Field has not been completed to date, Pirrung et al. [2004] and Carn [2000] both identified a radial distribution of vents around the Lamongan stratovolcano, with lineaments that overlap with those observed in the maar only dataset. This trend is also weakly apparent in maar-only maps (Figure 5).

3.3 Newer Volcanics Province

The Newer Volcanics Province contains 23 maars with complete rims and measurable elongation (Table 1). The maars of the NVP exhibit two strong modes and two weak modes in primary elongation orientation (Figure 6). The strong modes are 9–41° (P_A, $n = 10$) and 167–176° (P_B, $n = 3$). The weak modes range from 104–136° (P_C, $n = 5$) and 46–63° (P_D, $n = 3$). The faulting modes in NVP are 78–123° (F_A), 158-13° (F_B), and 123–140° (F_C). There are multiple maar-derived nearest neighbor direction modes: 108–132° (N_A), 132–132° (N_B), and 44–75° (N_C) supported by three or more maars in line with one another. Modes N_A and N_B are strong while mode N_C is weak. Of the primary maar elongation modes, the weak mode P_C is encompassed by faulting modes F_A and F_C, and nearest neighbor mode N_A. P_B correlates with faulting mode F_B. About half of mode P_A is encompassed by faulting mode F_B. Finally, primary elongation orientation mode P_D is encompassed by nearest neighbor mode N_C. Part of nearest neighbor mode N_C overlaps partially with the primary elongation orientation mode P_A. In the NVP, 18/23 maar primary elongation orientations share similar orientations with faulting and nearest neighbor orientation data. Including maars which are not part of maar modes, 20/23 maars are similar to faulting and nearest neighbor mode orientations. No published nearest neighbor analysis for NVP exists at the time of publication, but vent location data from Boyce [2013] were used to compute nearest neighbor orientations in the NVP, which shows a common orientation for nearest neighbor pairs at 90–120° and 30–60°

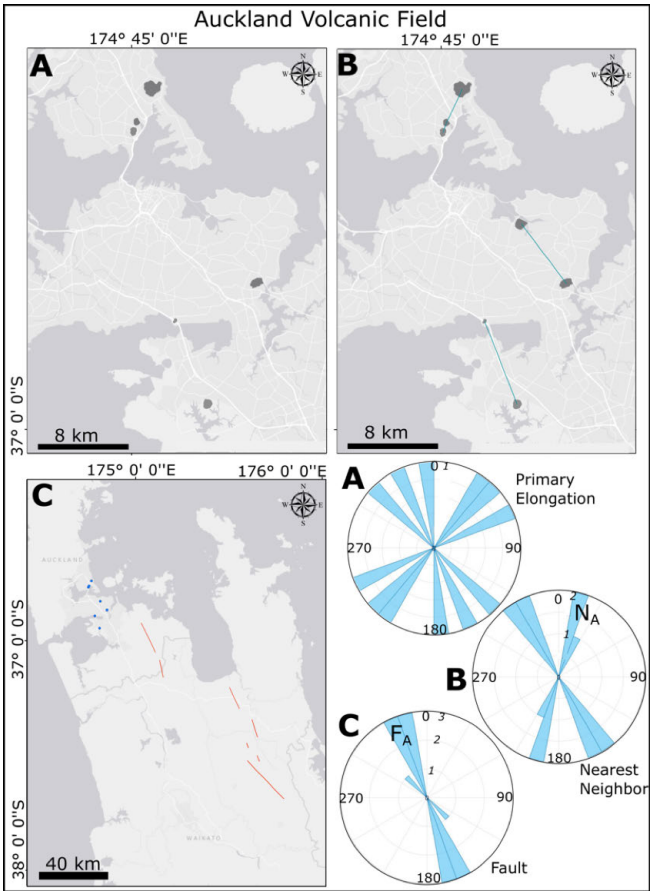

Figure 4: Auckland Volcanic Field spatial (map) and orientation data (rose diagram). [A] Maars measured for analysis of primary elongation orientation. Grey color indicates no maars occur in a mode. [B] Digitized maars with nearest neighbor lines between them. [C] Regional view where blue dots represent maars and red lines indicate mappable faults. Base map from ESRI and Open Street Map, WGS 1984.

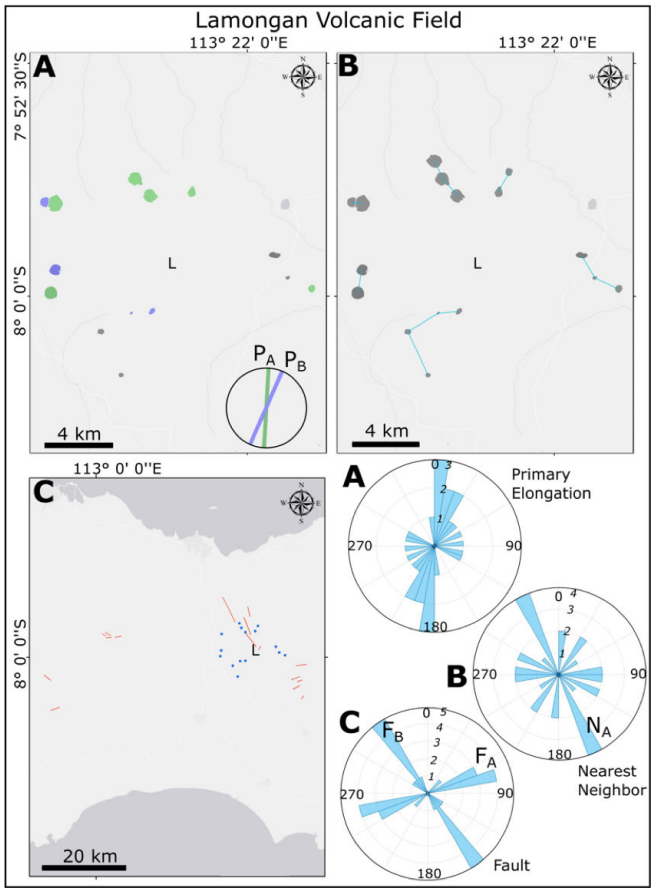

Figure 5: Lamongan Volcanic Field spatial (map) and orientation data (rose diagram). [A] Maars measured for primary elongation orientation. Colors reflect orientation modes Green (PA), Blue (PB), Grey (none). The summit of Lamongan Stratovolcano indicated by L. [B] Digitized maars and nearest neighbor lines. [C] Regional view with digitized maars (blue dots) and fault lines (red lines). Two maars in this field, Ranu Gunungparang and Ranu Gedang, were included in the nearest neighbor analysis, but excluded from primary orientation due to their circularity.

similar to observed maar alignments N_A and N_C.

3.4 Pali Aike Volcanic Field

The Pali Aike Volcanic Field contains 23 maars with measurable elongations. PAVF maars exhibit four strong modes in primary elongation orientation: 136–148° (P_A, $n = 5$), 1–13° (P_B, $n = 4$), 81–96° (P_C, $n = 4$), and 166–175° (P_D, $n = 4$, Figure 7). One weak primary elongation orientation mode exists at 108–125° (P_E, $n = 3$). Faulting data for PAVF exhibits three strong modes at 119–146° (F_A), 48–51° (F_B), and 71–74° (F_C). The maar-derived nearest neighbor data for Pali Aike exhibits three strong modes from 132–163° (N_A), 87–98° (N_B), and 98–110° (N_C), supported by three or more aligned maars. While primary elongation orientation mode P_B has no matching modes in faulting or nearest neighbor data, all other primary elongation orientation modes are met with a complimentary fault or nearest neighbor mode. Primary elongation orientation modes P_A and P_E both overlap with both faulting and nearest neighbor modes F_A and N_A. Primary elongation orientation mode P_C is matched in part by faulting mode F_C, but is entirely covered by nearest neighbor mode N_B. Primary elongation orientation mode P_D is similar to nearest neighbor mode N_A. Lastly, nearest neighbor mode N_A also encompasses primary elongation orientation mode P_F. Analysis of the all vents in the PAVF by Le Corvec et al. [2013b] using 467 volcanic features revealed 275 lineaments with two orientations (NW–SE, NE–SW) that correlate with regional strike slip and normal faults as was also shown by Mazzarini [2003]. This is consistent with elongation mode P_A composed of 5/23 PAVF maars. Qualitative observations of other complex features not included in maar orientation measurements because of mixed magmatic

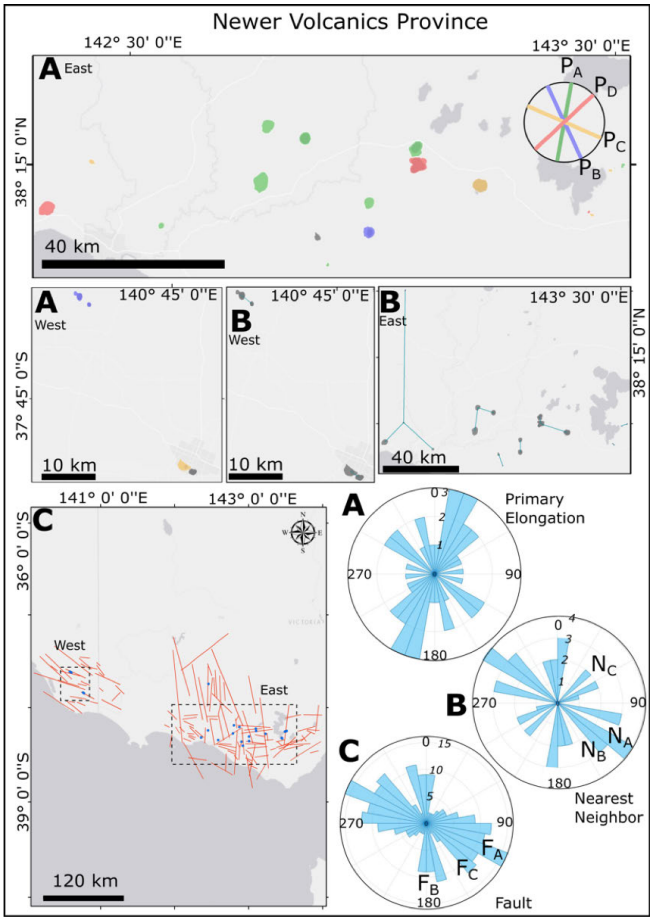

Figure 6: Newer Volcanics Province spatial (map) and orientation data (rose diagram). [A] all maars measured for primary elongation orientation. Maars in modes by color Green (PA), Blue (PB), Orange (PC), Red (PD), Grey (none). [B] Nearest neighbor lineaments between maars. [C] Location of all of the maars from a regional view (blue dots) and fault lines in the region (red lines) showing West and East subset areas from [A] and [B].

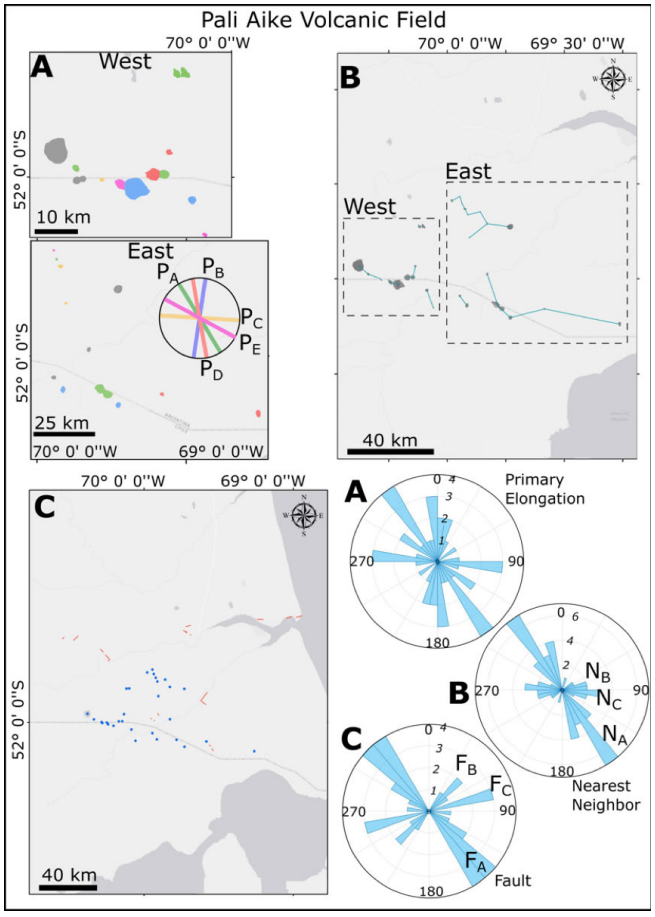

Figure 7: Pali Aike Volcanic field spatial (map) and orientation data (rose diagram).. [A] Maars measured for primary elongation orientation. Colors represent mode Green (PA), Blue (PB), Orange (PC), Red (PD), Pink (PE), Grey (none). [B] Nearest neighbor lines between all maars. Inset for A shown. [C] Maars (blue dots) and fault lines (red lines) from a regional view.

phreatomagmatic elements, also align with observed modes.

3.5 Pinacate Volcanic Field

The Pinacate Volcanic Field (PinVF) contains eight maars with measurable elongation orientations. The maars exhibit one strong mode in primary elongation orientation from 17–28° (P_A, $n = 3$; Figure 8). Faulting data were found to have one strong mode from 127–153° (F_A). Maar-derived nearest neighbor data exhibits one strong mode from 91–95° (N_A) supported by three or more aligned maars. The primary elongation orientation mode does not match faulting or nearest neighbor orientations. Faulting and nearest neighbor orientations do not match. Two maars not a part of any of the maar modes align with fault modes. Nearest Neighbor analysis by Le Corvec et al. [2013a] of 453 vents from PinVF revealed 38 individual vent lineaments with two different orientations (NNW–SSE and NE–SW). These broader trends correlate well with the regional strike slip faulting observed in both studies, but only two maars in modes had similar orientations of elongations to these trends.

3.6 The Maars of the Macolod Corridor

The Maars of the Macolod Corridor include 14 maars with measurable elongations. Primary maar elongation orientation data exhibits three strong modes (Figure 9) from 4–8° (P_A, $n = 3$), 31–40° (P_B, $n = 3$), and 60–70° (P_C, $n = 3$), and one weak mode from 97–114° (P_D, $n = 3$). There are three strong modes among the faulting data from 27-68° (F_A), 177-18° (F_B), and 90° (F_C). Three strong modes were found in maar-derived nearest neighbor data from 59–62° (N_A), and 153–161° (N_B) with at least three maars in a line. Each of the four maar modes have a similar faulting or nearest neighbor mode. Primary elongation orientation mode P_A ex-

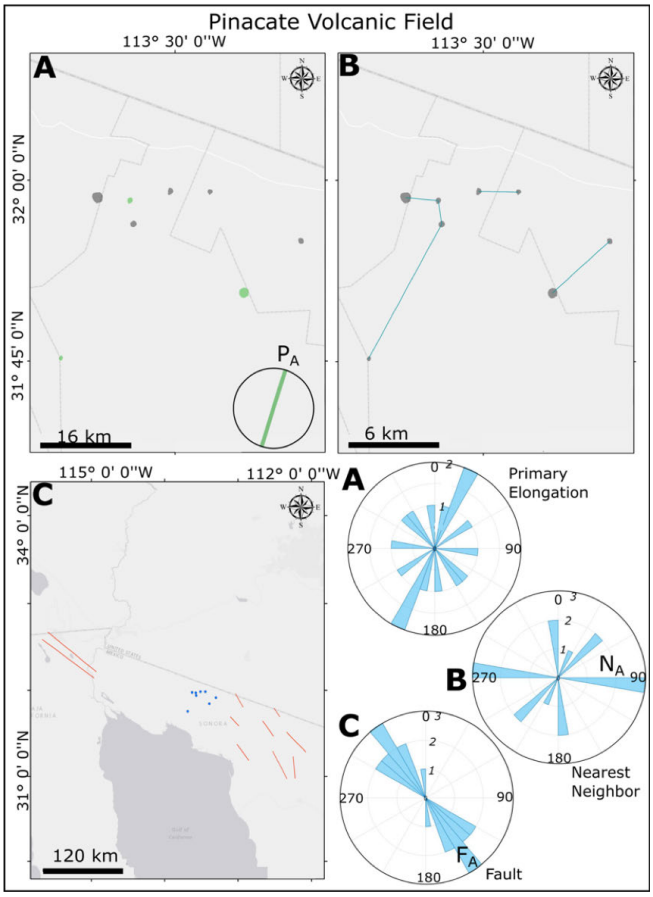

Figure 8: PinVF spatial (map) and orientation data (rose diagram). [A] Maars measured for primary elongation orientation. Color indicates modes Green (PA), Grey (none). [B] Nearest neighbor lines for maars. [C] Digitized maars (blue dots) and fault lines (red lines) from a regional view.

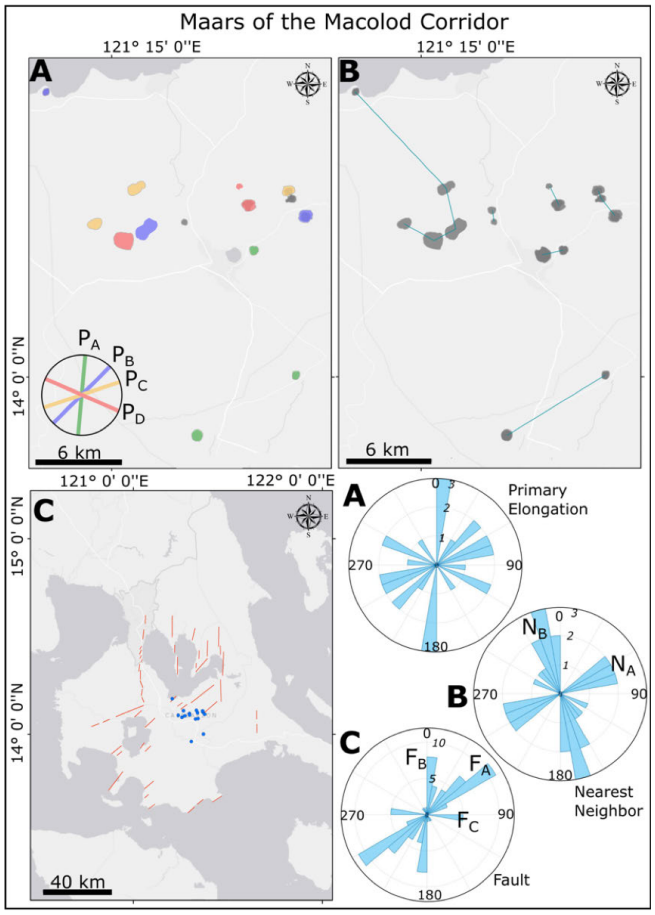

Figure 9: Maars of the Macolod Corridor spatial (map) and orientation data (rose diagram). [A] Maars measured for primary elongation orientation. Colors represent modes Green (PA), Blue (PB), Yellow (PC), Red (PD), Grey (none). [B] Nearest neighbor lines. [C] Location of maars from a regional view (blue dots) and fault lines in the region (red lines; Table 1).

hibits a similar orientation as faulting mode F_B. Faulting mode F_A shares a similar orientation with the maars of primary elongation orientation mode P_B. Primary elongation orientation mode P_C is similar to nearest neighbor mode N_A and faulting mode F_A. Primary orientation mode P_D has overlap with faulting mode F_C, but only for one maar's elongation orientation. In summary, there are 10/14 maars in modes with similar orientations as faulting or nearest neighbor data. If all maars are considered, regardless of maar modes, then 12/14 maars can be found with similar primary elongation orientations to faulting and nearest neighbor data. Nearest neighbor and faulting data also exhibit overlap in this field between modes F_A and N_A. The maars of the Macolod Corridor have less published data than the other fields and precise counts of the number of more vegetated vents (scoria cones, fissures etc.), and indeed the extent of the field relative to the surrounding stratovolcanoes is limited [Irapta 2018; LLDA 2014] so there was no available comprehensive vent alignment data.

3.7 Serdán Oriental Volcanic Field

The Serdán Oriental Volcanic Field contains nine maars with measurable elongations. One strong primary elongation orientation mode was found (Figure 10) from 70–77° (P_A, $n = 3$). Faulting data exhibits two strong modes from 118–154° (F_A) and 5–13° (F_B). No maar-derived nearest neighbor mode included three or more maars in a line. Three of the maars share similar primary elongation orientations as faulting, but do not fall under a maar mode. Analysis of all the vents within the SOVF has not been completed to date, likely due to the low number of individual vents within the field. The Aljojuca maar has been described as part of an east west alignment with older scoria cones [De León-Barragán et al. 2020]. This alignment, and the weak east-west nearest neighbor trend observed in the rose diagram (Figure 10), is consistent with regional east-west structures related to the Trans Mexican Volcanic Belt [Suter et al. 1992].

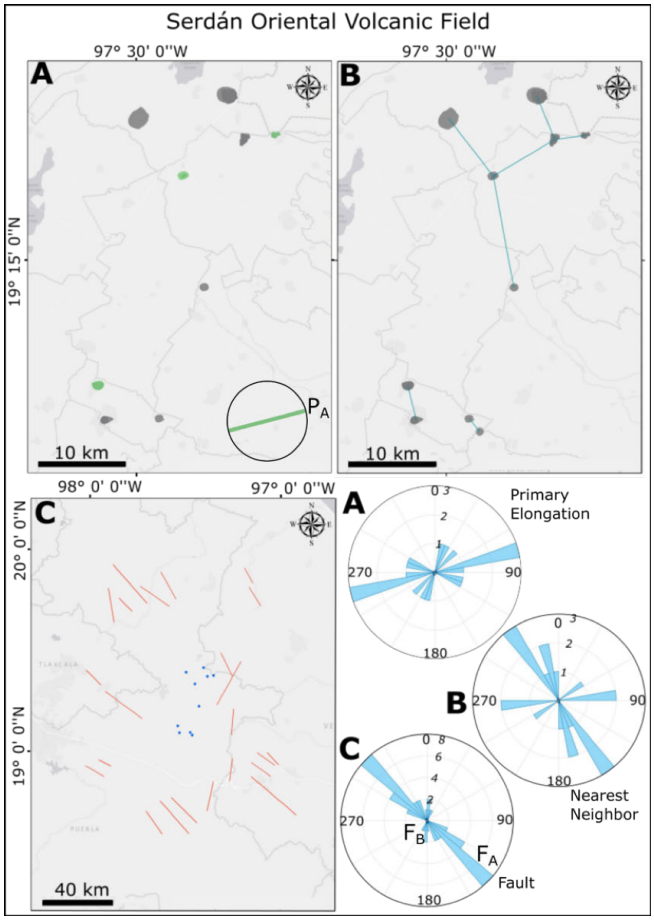

Figure 10: Serdán Oriental Volcanic Field spatial (map) and orientation data (rose diagram). [A] Maars measured for primary elongation orientation. Colors indicate maar modes Green (PA), Grey (none). [B] Maar only nearest neighbor lines. [C] Location of all maars from a regional view (blue dots) and fault lines in the region (red lines). The east west structures of the Trans Mexican Volcanic Belt are not visible in the study area (Table 1).

4 Discussion

The correlation between regional stress indicators and the geographic distribution and alignment of volcanic vents has been described for landforms in monogenetic fields, with a heavy bias on extensional settings [Cebriá et al. 2011; Connor et al. 1992; Corazzato and Tibaldi 2006; Hernando et al. 2014; Mazzarini 2003]. In some cases, the shape of the entire volcanic field can align with the regional stress field [Le Corvec et al. 2013b]. In the formation of mafic volcanic cones, vents, and maars, magma rises to the surface from an underground source by tabular dikes and sills frequently resulting in linear trends of vents at the surface. The shape of the resulting landforms is related to eruption history and external conditions like wind, but the process by which they are supplied magma is generally assumed to be the same at depth [Lorenz and Haneke 2004].

Research regarding dike propagation has shown that dikes within volcanic fields are often aligned with the regional tectonic stress field, that is, perpendicular to the least compressive stress [Acocella and Neri 2009]. This is because dikes can either utilize pre-existing faults as pathways to get magma to the surface, if the current stress regime is favorable, or create new pathways that are influenced by that stress regime [Gonnermann and Taisne 2015]. Since the distribution of features is determined by dike position and orientation, it is expected that maar craters would exhibit evidence of this regional stress control in their distribution. In this study faults in each field were compared with lineaments identified by nearest neighbor results of the maars alone, and all features in the field when available in published literature (Table 1). Six of the seven volcanic fields studied here were found to have nearest neighbor alignments composed of three or more maars (Auckland, Lamongan, Newer Volcanics Province, Pali Aike, Pinacate, and Macolod Corridor). Of the six fields where these maar-only lineaments were identified, four were found to have some overlap with faulting modes for those fields (Lamongan, Newer Volcanics Province, Pali Aike, and Macolod Corridor). Although exposed faulting can be limited by burial, and complicated by the presence of faults related to different stress regimes than those present during the eruption of the volcanic landforms of interest, there was a measurable overlap between nearest neighbor and faulting data supporting their use as a stress indicator. While nearest neighbor analysis using only maars is limited by the sample size, the maar-only lineaments correlate with whole field nearest neighbor analyses from the literature, even for fields with limited maar-only lineaments. This agreement is indicative of the consistency of this phenomena in the fields studied. Maars have a geographic distribution predominantly controlled by the regional stress regime, just as scoria cones do, the only difference being that the conditions at maars enabled phreatomagmatic explosions. This suggests similar controls on magma transport at depth for both scoria cones and maars. This relationship is necessary to establish before investigating the influence of regional stress on the shape of these landforms.

The presence of elongation in maar craters is a documented characteristic, typical of the volcanic feature, and is related to lateral migration of explosion locations during an eruption [De León-Barragán et al. 2020; Graettinger 2018; Ort and Carrasco-Núñez 2009]. However, the controls on this lateral migration have not yet been investigated for a large population of maars. For this study, less than 5 % of the maars with crater rims were too circular to identify an orientation, further highlighting the commonality of lateral migration. Of the maars which exhibit elongation, 74 % fall within elongation modes within their field. When just the strong modes are considered, 55 % of all maars are part of primary elongation orientation modes. These

percentages are biased by fields where this trend is strongest (Newer Volcanics Province and Pali Aike). Although not every maar presents an elongation orientation that correlates to a mode, these data indicate a commonality within some of the volcanic fields studied and might suggest a consistent influence on crater growth in these fields.

The volcanic fields analyzed can be categorized into three distinct groups based on the observed relationship between maar orientation, orientation modes, and regional stress indicators (Figure 11). The first group includes Pali Aike, Newer Volcanics Province, and the maars of the Macolod Corridor, which each have high numbers of maars that share similar primary elongation orientations as well as large numbers of maars that match faulting and nearest neighbor orientations. The second group contains Lamongan Volcanic Field, which has many maars that share primary elongation orientations, but has no maars which match nearest neighbor or faulting. Finally, the third group of Auckland, Pinacate, and Serdán Oriental Volcanic Field have a limited number of maars sharing similar primary elongation orientations and only a few primary maar elongations that match faulting or nearest neighbor data. Each of these three groups possesses distinguishing features, besides the number of maars that fall in modes, which group them together and set them apart from the others.

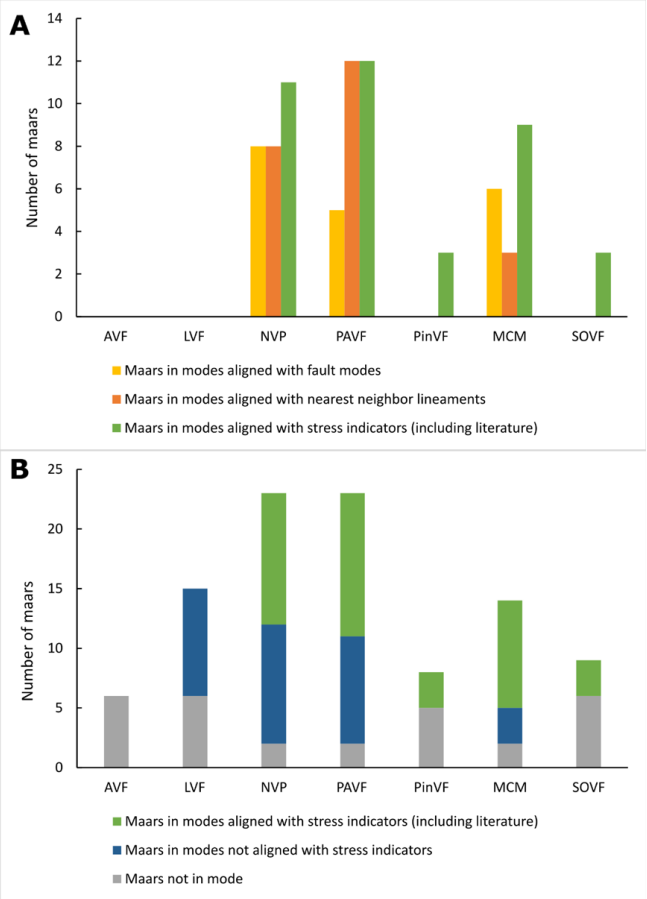

Figure 11: Comparison of modes and alignment across the seven volcanic fields. [A] Number of maars in modes aligned with different stress indicators. [B] Number of maars in and out of modes aligned with stress indicators.

The first group is comprised of fields which have both high numbers of maars in primary elongation orientation modes (Newer Volcanics Province, Pali Aike, and Macolod Corridor; average 82 % of maars in modes), and high numbers of those maars which share similar primary elongation orientations with regional stress indicators (average 82 % of each field; Table 1). The correlation between maar distribution, faults and lineaments show a strong reginal stress influence on the geographic distribution of volcanic features. Within the Newer Volcanics Province, there are multiple examples of maars whose locations are directly collocated with faults (Figure 12). However, of the nine maars collocated with faults, the primary elongation orientation of the maar never matches the coincident fault. Further, while many maars can be found with primary elongation orientations similar to the orientation of faults and nearest neighbor lineaments in the Newer Volcanics Province, these maars within a lineament do not have an orientation of elongation similar to the lineament (Figure 6 and 11). In the PAVF and MCM the majority of maars in lineaments do not have orientations similar to the lineament (Figure 7 and 9). NVP and PAVF are both intraplate monogenetic fields, while MCM is in an extensional province surrounded by large stratovolcano and caldera volcanoes related to dual subduction around the Philippines. The similarity of maar primary elongation orientations with regional stress indicators, without spatial correlation to lineaments was unexpected. Of all the volcanic fields, only 18 % of maars found in lineaments shared a primary elongation orientation with the lineament they composed (Figure 13A). This indicates that the elongation of maars in these fields is not simply the result of explosion locations migrating along a feeder dike in line with regional stress patterns.

The Lamongan Volcanic Field is considered its own group and contains fourteen maars. Of those maars, 71 % fall within primary elongation orientation modes. However, unlike the other three fields which exhibit high populations of maars within primary elongation orientation modes, none of Lamongan's maar orientation modes overlap with faulting or nearest neighbor modes (Figures 5 and 11). Furthermore, only one maar (not in a mode) can be found with a primary elongation orientation that matches that of a faulting mode (Figure 5). The nearest neighbor mode for this field is matched by faulting but has no maars which share its orientation. The Lamongan Volcanic Field sits within the Sunda Arc and contains a large multivent stratovolcano with monogenetic cones and maars on its flanks. As observed by other researchers [Carn

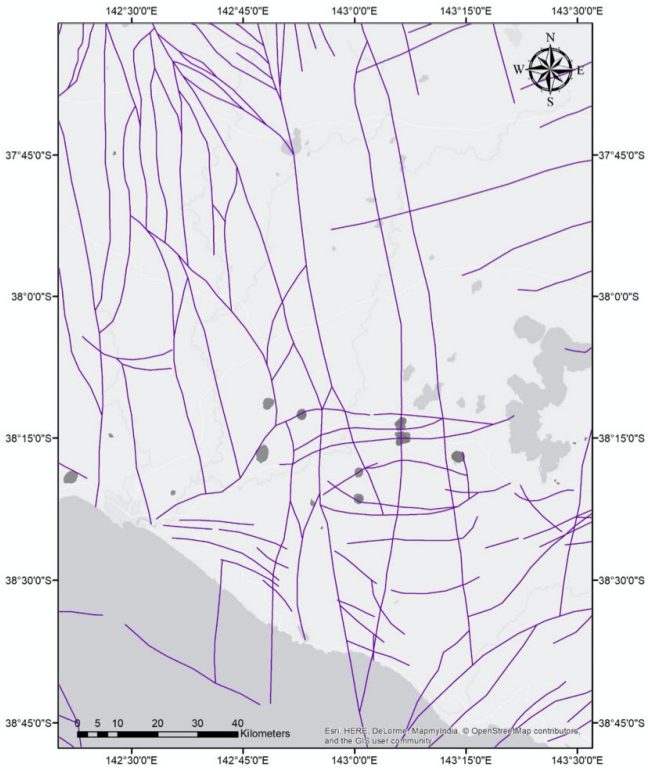

Figure 12: Faulting along the western side of the Newer Volcanic Province (Australia). Several maars are intersected by faults but do not have primary elongation orientations that match the fault. Data from Boyce [2013].

2000; Pirrung et al. 2004], the Lamongan Volcanic Field has a radial distribution of the smaller volcanic landforms, including maars, relative to this central construct. While the maars have orientations that cover all the major directions, they do not have elongation orientations that point back at Lamongan Volcano (Figure 5). The presence of the volcano may have influenced the local stress regime and overridden more regional stresses [Acocella and Neri 2009] influencing dike propagation, and thus the distribution of features. However, it does not appear to explain the orientation of maar elongation. These observations suggest that within Lamongan Volcanic Field, maar elongation orientations are not influenced by regional or local crustal stresses.

The fields in group three, Auckland, Pinacate, and Serdán Oriental, each have fewer than ten maars with measurable elongation orientations (the lowest counts found in this study). In all three fields, no maars occur in modes that match faulting or nearest neighbor modes (Figure 11). Individual maars not in modes do occur within lineaments of vents [De León-Barragán et al. 2020; Le Corvec et al. 2013a; Le Corvec et al. 2013b]. However, the majority of maars in these fields do not have orientations of elongation that align with these stress indicators. These fields all exhibit the lowest number of maars in modes, ranging from 0–37 %. All three fields are intraplate monogenetic fields, although Serdán Oriental is notably the only field with rhyolitic maars in this study. It is possible that the root cause of the lack in modes belongs to their shared low number of maars.

In order for any orientation mode to be identified in this methodology, even a weak one, three or more data points must be found within twenty degrees of one another. While this is an easy requirement to meet for other fields, in these three, a mode would have to contain more than 30 % of the maars measured. Across all fields, the average primary elongation orientation mode contains only 22 % of the maars in field. In spite of the low numbers, the group three volcanic fields contained maars with primary elongations which covered a wide range of orientations and none of the fields were found to have a majority of maar elongation orientations in any single orientation (Figures 4, 8 and 10). Group three maars may be small in number but indicate that regional stress was not the main influence on the majority of maar crater elongations.

More than half of the maars in the volcanic fields studied exhibit similar elongation orientations as faulting and nearest neighbor trends, but only 18 % of maars found in nearest neighbor lineaments shared a primary elongation orientation with the lineament they composed (Figure 13A). This has been noted in the study of individual maars, such as Joya Honda in the Ventura Volcanic Field in Mexico, which occurs within a line of aligned vents, but where the crater shape is not aligned in the same direction [López Loera et al. 2008]. Similarly, observations of eroded diatremes like Ship Rock in New Mexico reveal many dikes that are offset from the main diatreme. These observations suggest that for many maars the stresses that determine an individual maar's geographic position are not the same as those acting on crater elongation. The apparent inconsistency between similar orientations of elongation within a volcanic field (on average 84 % of maars occur within modes), the lack of spatial clustering of maars in modes, and the lack of correlation of orientation in maars within a given lineament presents a challenge for narrowing down the forces influencing elongation of maars.

To analyze the azimuthal distribution of maar modes and stress indicators, the percentage of potential orientations (as a factor of 360 degrees) for maar primary elongations and stress indicators were tabulated (Figure 13B). All of the fields have maar crater orientations that cover <50 % of the available orientations, while the orientation of stress indicators within individual fields varies from 11–71 % (33–94 % if allowed a 10 degree buffer). The sheer range of orientations accounted for in each field by nearest neighbor and faulting data almost always surpasses the percentage of maars for that field which were found to share a similar primary elongation orientation with those orientations. Interestingly, Lamongan's stress indicators correlated with the gap in maar orientations (Figure 5). In summary, maar elon-

gations have more limited orientations, compared to stress indicators across fields, and maars do not appear to have purely random orientations.

If regional structural controls were the dominant influence on the elongation orientation of maar craters in general, a much larger portion of the maars in each field would be found with similar elongation orientations as faults and nearest neighbor lineaments. Although not analyzed due to low occurrence, each volcanic field studied had at least one maar that displayed more than one direction of elongation and a convoluted shape, but Bullen Meri of the Newer Volcanics Province shows that this second orientation also does not necessarily correlate with regional faults (Figure 1B). For those maars where regional stress does not correlate with primary crater elongation, laterally migrating phreatomagmatic explosions are likely influenced by more local controls related to the host geology, variations in the plumbing system at shallow levels, and stresses influenced by the eruption itself.

Although the fields studied here occur in a range of tectonic settings, the majority occur in extensional basins with surficial coverage of pyroclastic and sedimentary rocks overlaying thicker sequences of sedimentary rocks or a crystalline basement. Host lithologies influence the distribution, orientation, and character of aquifers that rising magma may encounter to produce phreatomagmatism. Variation in water availability can lead to multiple explosion foci or migration of foci over the course of an eruption and has been cited as a likely source of lateral migration in studies of individual maars [Le Corvec et al. 2018; Lorenz 2003; Ort and Carrasco-Núñez 2009; White and Ross 2011], suggesting that maar elongation may partly reflect aquifer geometry rather than dike geometry.

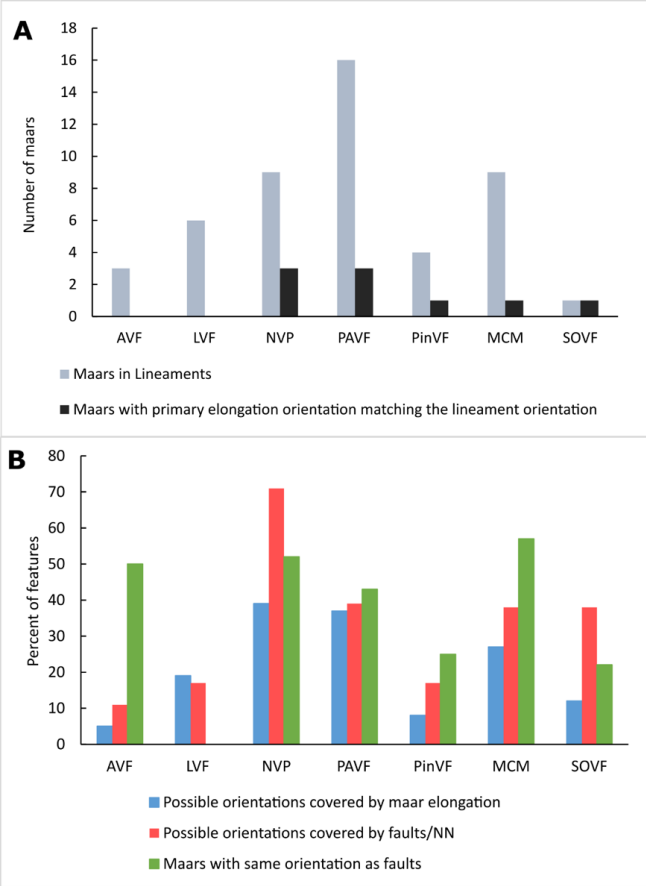

Figure 13: Comparisons of maar orientations relative to other metrics to contextualize the results. [A] The occurrence of maars in lineaments and how many of those maars have primary elongations that match the lineament. [B] Comparison of the percent of possible orientations (out of 360 degrees) of maar orientations and stress indicators.

Additionally, the occurrence of maars in unconsolidated or weak strata may influence the shape of maars. Research into the influence of host rock strength on the size and shape of maars [Auer et al. 2007; Macorps et al. 2016] has focused on crater stability during growth. For example, in the case of Joya Honda the crater shape asymmetry was attributed to tilted strata on one side of the crater being undercut by the crater and encouraging asymmetrical mass wasting [López Loera et al. 2008]. Material properties of host rocks (density, strength, contrasts), not only contribute to the (in)stability of a crater, but also influences the propagation of magma. For instance, shallow sill complexes primarily form when dikes encounter the contact between areas of strongly contrasting rigidity [van den Hove et al. 2017]. Although distribution of different lithologies around and beneath maar volcanoes requires more individualized studies than this work allows, the majority of the volcanic fields analyzed here are hosted in weak strata atop bedrock. Therefore, the commonality of elongation orientations within larger volcanic fields may be related to these host rock contrasts and to the occurrence of sills within maar feeder systems. These can contribute to the lateral migration of explosion locations in some maar forming eruptions. Work in the Hopi Buttes, an eroded monogenetic field that contains numerous maar-diatreme structures, demonstrated the prevalence of sill-like structures at various depths within the sedimentary host rock sequence [Muirhead et al. 2016; Re et al. 2015; Valentine et al. 2017]. Additional investigations into the geometry and inclination of feeder dikes and sills relative to crater shape may provide insight into individual maars and their final crater geometry.

In addition to the static conditions before an eruption, recent work has drawn attention to the influence of the dynamic forces resulting from the subsurface explosive activity that drives maar formation itself [Le Corvec et al. 2018]. The supply of magma and water, and host rock material properties likely vary in direct response to the eruption itself. Numerical studies by Le Corvec et al. [2018] indicate that the initial explosion of a maar eruption could alter the stress field around the maar-diatreme and divert the dike which

feeds it. This change in stress field, and dike diversion, would influence the elongation orientation of maars. Further research into the response of aquifers to rising magma and partially confined subsurface explosions would shed additional light on the influences on lateral explosion migration during a maar-forming eruption.

5 Conclusions

This study investigated the orientation of elongated maars across seven locations in monogenetic and complex volcanic fields. Across these fields only 31 % of maars showed a correlation between the orientation of the maar crater and regional stress indicators. Of the fields studied, three showed a higher correlation between maar orientation and the regional stress indicators (Newer Volcanics Province, Pali Aike Volcanic Field and the Macolod Corridor), but for maars that occurred within a lineament of volcanic vents the elongation of the crater rarely (18 %) aligned with the lineament. Furthermore, maars which shared similar primary elongation orientations with other maars were not found to be grouped close together geographically. The tendency of maars to exhibit similar primary elongation orientations within a field, but not with proximal maars or maars within the same lineament, suggest the regional stresses that influence a feeder dike's propagation do not strongly control the elongation of maar craters. The evolution of conceptual models of maar formation, based on recent field and numerical research, suggest that the formation of sills, and dynamic stress regimes produced by the eruption itself, should be considered alongside localized variation in the hydrology and rock strength as influences on the lateral migration of explosion locations during a maar forming eruption.

Additional research focused on the study of diatreme shapes using eroded diatremes and geophysical evidence, the hydrologic conditions that led to past maar eruptions, shallow geologic units, and the response of water and water-saturated sediments to the intrusion of magma, are necessary to constrain the influences on lateral migration of phreatomagmatic explosions during maar-forming eruptions. Hazard analyses for future maar forming eruptions in populated volcanic fields such as Auckland and the Macolod Corridor would benefit from the ability to anticipate the possibility and direction of lateral migration during an eruption.

Acknowledgements

We would like to thank Julie Boyd, Jozua van Otterloo, and Fancesco Mazzarini for providing access to their structural and vent location data for the Newer Volcanics Province and Pali Aike, respectively. This work was funded through internal University of Missouri-Kansas City research funds to A. Graettinger. We are grateful to Pierre-Simon Ross for his constructive feedback on an early version of this manuscript. N. Irapta provided valuable insight into the Macolod Corridor. We also thank K. Németh and B. van Wyk de Vries valuable reviews, and Pierre Delmelle for their editorial oversight.

Author contributions

This manuscript represents the results of C. Nichols' masters thesis at the University of Missouri Kansas City. Data collection, analysis and manuscript drafting were accomplished by C. Nichols. Graettinger conceived of and supervised the research and contributed to manuscript writing and editing.

Data availability

The data on maar shape is derived from the MaarVLS shape database available on Vhub.org. Maar elongation orientation data is also available at Vhub.org.

Copyright notice

References

Acocella, V. and M. Neri (2009). "Dike propagation in volcanic edifices: Overview and possible developments". *Tectonophysics* 471.1-2, pp. 67–77. ISSN: 0040-1951. DOI: 10.1016/j.tecto.2008.10.002.

Acocella, V., T. Korme, F. Salvini, and R. Funiciello (2003). "Elliptic calderas in the Ethiopian Rift: control of pre-existing structures". *Journal of Volcanology and Geothermal Research* 119.1-4, pp. 189–203. DOI: 10.1016/s0377-0273(02)00342-6.

Auer, A., U. Martin, and K. Németh (2007). "The Fekete-hegy (Balaton Highland Hungary) "soft-substrate" and "hard-substrate" maar volcanoes in an aligned volcanic complex – Implications for vent geometry, subsurface stratigraphy and the palaeoenvironmental setting". *Journal of Volcanology and Geothermal Research* 159.1-3, pp. 225–245. ISSN: 0377-0273. DOI: 10.1016/j.jvolgeores.2006.06.008.

Boyce, J. (2013). "The Newer Volcanics Province of southeastern Australia: a new classification scheme

and distribution map for eruption centres". *Australian Journal of Earth Sciences* 60.4, pp. 449–462. issn: 1440-0952. doi: 10.1080/08120099.2013.806954.

Carn, S. A. (1999). "Application of synthetic aperture radar (SAR) imagery to volcano mapping in the humid tropics: a case study in East Java, Indonesia". *Bulletin of Volcanology* 61.1-2, pp. 92–105. issn: 1432-0819. doi: 10.1007/s004450050265.

– (2000). "The Lamongan volcanic field, East Java, Indonesia: physical volcanology, historic activity and hazards". *Journal of Volcanology and Geothermal Research* 95.1-4, pp. 81–108. doi: 10.1016/s0377-0273(99)00114-6.

Carrasco-Núñez, G., M. H. Ort, and C. Romero (2007). "Evolution and hydrological conditions of a maar volcano (Atexcac crater, Eastern Mexico)". *Journal of Volcanology and Geothermal Research* 159.1-3, pp. 179–197. issn: 0377-0273. doi: 10.1016/j.jvolgeores.2006.07.001.

Cassidy, J. and C. A. Locke (2010). "The Auckland volcanic field, New Zealand: Geophysical evidence for structural and spatio-temporal relationships". *Journal of Volcanology and Geothermal Research* 195.2-4, pp. 127–137. issn: 0377-0273. doi: 10.1016/j.jvolgeores.2010.06.016.

Cebriá, J., C. Martın-Escorza, J. López-Ruiz, D. Morán-Zenteno, and B. Martiny (2011). "Numerical recognition of alignments in monogenetic volcanic areas: Examples from the Michoacán-Guanajuato Volcanic Field in Mexico and Calatrava in Spain". *Journal of Volcanology and Geothermal Research* 201.1-4, pp. 73–82. issn: 0377-0273. doi: 10.1016/j.jvolgeores.2010.07.016.

Connor, C. B., C. D. Condit, L. S. Crumpler, and J. C. Aubele (1992). "Evidence of regional structural controls on vent distribution: Springerville Volcanic Field, Arizona". *Journal of Geophysical Research* 97.B9, p. 12349. doi: 10.1029/92jb00929.

Corazzato, C. and A. Tibaldi (2006). "Fracture control on type, morphology and distribution of parasitic volcanic cones: An example from Mt. Etna, Italy". *Journal of Volcanology and Geothermal Research* 158.1-2, pp. 177–194. issn: 0377-0273. doi: 10.1016/j.jvolgeores.2006.04.018.

D'Orazio, M., S. Agostini, F. Mazzarini, F. Innocenti, P. Manetti, M. J. Haller, and A. Lahsen (2000). "The Pali Aike Volcanic Field, Patagonia: slab-window magmatism near the tip of South America". *Tectonophysics* 321.4, pp. 407–427. doi: 10.1016/s0040-1951(00)00082-2.

De León-Barragán, L., G. Carrasco-Núñez, and M. H. Ort (2020). "Stratigraphy and evolution of the Holocene Aljojuca Maar volcano (Serdán-Oriental basin, Eastern Trans-Mexican Volcanic Belt), and implications for hazard assessment". *Journal of Volcanology and Geothermal Research* 392, p. 106789. issn: 0377-0273. doi: 10.1016/j.jvolgeores.2020.106789.

Defant, M. J., J. Z. D. Boer, and O. Dietmar (1988). "The western Central Luzon volcanic arc, the Philippines: two arcs divided by rifting?" *Tectonophysics* 145.3-4, pp. 305–317. doi: 10.1016/0040-1951(88)90202-8.

Ferrari, L., S. Conticelli, G. Vaggelli, C. M. Petrone, and P. Manetti (2000). "Late Miocene volcanism and intra-arc tectonics during the early development of the Trans-Mexican Volcanic Belt". *Tectonophysics* 318.1-4, pp. 161–185. doi: 10.1016/s0040-1951(99)00310-8.

Förster, H., D. Oles, U. Knittel, M. J. Defant, and R. C. Torres (1990). "The Macolod Corridor: A rift crossing the Philippine island arc". *Tectonophysics* 183.1-4, pp. 265–271. doi: 10.1016/0040-1951(90)90420-d.

García-Abdeslem, J. and T. Calmus (2015). "A 3D model of crustal magnetization at the Pinacate Volcanic Field, NW Sonora, Mexico". *Journal of Volcanology and Geothermal Research* 301, pp. 29–37. issn: 0377-0273. doi: 10.1016/j.jvolgeores.2015.05.001.

Germa, A., L. J. Connor, E. Cañon-Tapia, and N. Le Corvec (2013). "Tectonic and magmatic controls on the location of post-subduction monogenetic volcanoes in Baja California, Mexico, revealed through spatial analysis of eruptive vents". *Bulletin of Volcanology* 75.12. issn: 1432-0819. doi: 10.1007/s00445-013-0782-6.

Gonnermann, H. and B. Taisne (2015). "Magma Transport in Dikes". *The Encyclopedia of Volcanoes*, pp. 215–224. doi: 10.1016/b978-0-12-385938-9.00010-9.

Graettinger, A. (2018). "Trends in maar crater size and shape using the global Maar Volcano Location and Shape (MaarVLS) database". *Journal of Volcanology and Geothermal Research* 357, pp. 1–13. doi: 10.1016/j.jvolgeores.2018.04.002.

Gutmann, J. (2002). "Strombolian and effusive activity as precursors to phreatomagmatism: eruptive sequence at maars of the Pinacate volcanic field, Sonora, Mexico". *Journal of Volcanology and Geothermal Research* 113.1-2, pp. 345–356. doi: 10.1016/s0377-0273(01)00265-7.

Haller, M. J. and K. Németh (2006). "Architecture and pyroclastic succession of a small Quaternary (?) maar in the Pali Aike Volcanic Field, Santa Cruz, Argentina". *Zeitschrift der Deutschen Gesellschaft für Geowissenschaften* 157.3, pp. 155–164. doi: 10.1127/1860-1804/2006/0157-0467.

Hernando, I., J. Franzese, E. Llambıas, and I. Petrinovic (2014). "Vent distribution in the Quaternary Payún Matrú Volcanic Field, western Argentina: Its relation to tectonics and crustal structures". *Tectonophysics* 622, pp. 122–134. issn: 0040-1951. doi: 10.1016/j.tecto.2014.03.003.

Hopkins, J. L. et al. (2020). "Auckland Volcanic Field magmatism, volcanism, and hazard: a review". *New*

Zealand Journal of Geology and Geophysics, pp. 1–22. DOI: 10.1080/00288306.2020.1736102.

Irapta, P. N. S. A. (2018). "Morphologic characterization of the Macolod Corridor, Philippines Using Interferometric Synthetic Aperture Radar Digital Terrain Model Towards a Comprehensive Risk Analysis". MA thesis. University of Clermont-Ferrand, Clermont-Ferrand, France.

Jordan, S., R. Cas, and P. Hayman (2013). "The origin of a large (3km) maar volcano by coalescence of multiple shallow craters: Lake Purrumbete maar, southeastern Australia". *Journal of Volcanology and Geothermal Research* 254, pp. 5–22. DOI: 10.1016/j.jvolgeores.2012.12.019.

Kenny, J., J. Lindsay, and T. Howe (2012). "Post-Miocene faults in Auckland: insights from borehole and topographic analysis". *New Zealand Journal of Geology and Geophysics* 55.4, pp. 323–343. DOI: 10.1080/00288306.2012.706618.

Kereszturi, G., K. Németh, S. J. Cronin, J. Procter, and J. Agustın-Flores (2014). "Influences on the variability of eruption sequences and style transitions in the Auckland Volcanic Field, New Zealand". *Journal of Volcanology and Geothermal Research* 286, pp. 101–115. ISSN: 0377-0273. DOI: 10.1016/j.jvolgeores.2014.09.002.

Kharazizadeh, N., W. Schellart, J. Duarte, and M. Hall (2017). "Influence of lithosphere and basement properties on the stretching factor and development of extensional faults across the Otway Basin, southeast Australia". *Marine and Petroleum Geology* 88, pp. 1059–1077. ISSN: 0264-8172. DOI: 10.1016/j.marpetgeo.2017.08.034.

Ku, Y.-P., C.-H. Chen, S.-R. Song, Y. Iizuka, and J. J.-S. Shen (2009). "A 2 Ma record of explosive volcanism in southwestern Luzon: Implications for the timing of subducted slab steepening". *Geochemistry, Geophysics, Geosystems* 10.6. ISSN: 1525-2027. DOI: 10.1029/2009gc002486.

Laguna Lake Development Authority (2014). *Pandin Lake Development and Management Plan*. URL: http://llda.gov.ph/wp-content/uploads/dox/pandin-lake-dmp/pandin-lake-mgt-devt-plan.pdf (visited on 08/30/2018).

Langridge, R., W. Ries, N. Litchfield, P. Villamor, R. Van Dissen, D. Barrell, M. Rattenbury, D. Heron, S. Haubrock, D. Townsend, and et al. (2016). "The New Zealand Active Faults Database". *New Zealand Journal of Geology and Geophysics* 59.1, pp. 86–96. ISSN: 1175-8791. DOI: 10.1080/00288306.2015.1112818.

Le Corvec, N., M. S. Bebbington, J. M. Lindsay, and L. E. McGee (2013a). "Age, distance, and geochemical evolution within a monogenetic volcanic field: Analyzing patterns in the Auckland Volcanic Field eruption sequence". *Geochemistry, Geophysics, Geosystems* 14.9, pp. 3648–3665. ISSN: 1525-2027. DOI: 10.1002/ggge.20223.

Le Corvec, N., J. D. Muirhead, and J. D. L. White (2018). "Shallow magma diversions during explosive diatreme-forming eruptions". *Nature Communications* 9.1. ISSN: 2041-1723. DOI: 10.1038/s41467-018-03865-x.

Le Corvec, N., K. B. Spörli, J. Rowland, and J. Lindsay (2013b). "Spatial distribution and alignments of volcanic centers: Clues to the formation of monogenetic volcanic fields". *Earth-Science Reviews* 124, pp. 96–114. DOI: 10.1016/j.earscirev.2013.05.005.

Lesti, C., G. Giordano, F. Salvini, and R. Cas (2008). "Volcano tectonic setting of the intraplate, Pliocene-Holocene, Newer Volcanic Province (southeast Australia): Role of crustal fracture zones". *Journal of Geophysical Research* 113.B7. ISSN: 0148-0227. DOI: 10.1029/2007jb005110.

Lindsay, J., G. Leonard, E. Smid, and B. Hayward (2011). "Age of the Auckland Volcanic Field: a review of existing data". *New Zealand Journal of Geology and Geophysics* 54.4, pp. 379–401. DOI: 10.1080/00288306.2011.595805.

López Loera, H., J. J. Aranda-Gómez, J. A. Arzate-Flores, and R. S. Molina-Garza (2008). "Geophysical surveys of the Joya Honda maar (México) and surroundings; volcanic implications". *Journal of Volcanology and Geothermal Research* 170.3-4, pp. 135–152. ISSN: 0377-0273. DOI: 10.1016/j.jvolgeores.2007.08.021.

Lorenz, V. (2003). "Maar-Diatreme Volcanoes, their Formation, and their Setting in Hard-rock or Soft-rock Environments". *GeoLines* 15, pp. 72–83.

Lorenz, V. and J. Haneke (2004). "Relationship between diatremes, dykes, sills, laccoliths, intrusive-extrusive domes, lava flows, and tephra deposits with unconsolidated water-saturated sediments in the late Variscan intermontane Saar-Nahe Basin, SW Germany". *Geological Society, London, Special Publications* 234.1, pp. 75–124. ISSN: 2041-4927. DOI: 10.1144/gsl.sp.2004.234.01.07.

Maccaferri, F., V. Acocella, and E. Rivalta (2015). "How the differential load induced by normal fault scarps controls the distribution of monogenic volcanism". *Geophysical Research Letters* 42.18, pp. 7507–7512. ISSN: 1944-8007. DOI: 10.1002/2015gl065638.

Macorps, É., A. H. Graettinger, G. A. Valentine, P.-S. Ross, J. D. L. White, and I. Sonder (2016). "The effects of the host-substrate properties on maar-diatreme volcanoes: experimental evidence". *Bulletin of Volcanology* 78.4. ISSN: 1432-0819. DOI: 10.1007/s00445-016-1013-8.

Mazzarini, F. (2003). "Spatial distribution of cones and satellite-detected lineaments in the Pali Aike Volcanic Field (southernmost Patagonia): insights into the tectonic setting of a Neogene rift system". *Journal of Volcanology and Geothermal Research* 125.3-4, pp. 291–305. DOI: 10.1016/s0377-0273(03)00120-3.

Mortimer, N. et al. (2014). "High-level stratigraphic scheme for New Zealand rocks". *New Zealand Jour-*

nal of Geology and Geophysics 57.4, pp. 402–419. doi: 10.1080/00288306.2014.946062.

Muirhead, J. D., A. R. Van Eaton, G. Re, J. D. L. White, and M. H. Ort (2016). "Monogenetic volcanoes fed by interconnected dikes and sills in the Hopi Buttes volcanic field, Navajo Nation, USA". *Bulletin of Volcanology* 78.2. issn: 1432-0819. doi: 10.1007/s00445-016-1005-8.

Ort, M. H. and G. Carrasco-Núñez (2009). "Lateral vent migration during phreatomagmatic and magmatic eruptions at Tecuitlapa Maar, east-central Mexico". *Journal of Volcanology and Geothermal Research* 181.1-2, pp. 67–77. issn: 0377-0273. doi: 10.1016/j.jvolgeores.2009.01.003.

Padilla, R., R. Sánchez, I. Domınguez Trejo, A. López Azcárraga, J. Mota Nieto, A. Fuentes Menes, F. Rosique Naranjo, E. Germán Castelán, and S. Campos Arriola (2013). *National Autonomous University of Mexico Tectonic Map of Mexico GIS Project*. http://www.datapages.com/gis-map-publishing-program/gis-open-files/geographic/tectonic-map-of-mexico-2013. doi: 10.4225/13/511C71F8612C3. [dataset].

Pirrung, M., G. Buchel, D. Merten, H. Assing, U. Schulte-Vieting, S. Heublein, M. Theune-Hobbs, and B. Boehrer (2004). "Morphometry, limnology, hydrology and sedimentology of maar lakes in East Java, Indonesia". *Studia Quaternaria* 21, pp. 139–152.

Re, G., J. White, and M. Ort (2015). "Dikes, sills, and stress-regime evolution during emplacement of the Jagged Rocks Complex, Hopi Buttes Volcanic Field, Navajo Nation, USA". *Journal of Volcanology and Geothermal Research* 295, pp. 65–79. issn: 0377-0273. doi: 10.1016/j.jvolgeores.2015.01.009.

Robertson, E. A. M., J. Biggs, K. V. Cashman, M. A. Floyd, and C. Vye-Brown (2015). "Influence of regional tectonics and pre-existing structures on the formation of elliptical calderas in the Kenyan Rift". *Geological Society, London, Special Publications* 420.1, pp. 43–67. issn: 2041-4927. doi: 10.1144/sp420.12.

Ross, P.-S., G. Carrasco-Núñez, and P. Hayman (2017). "Felsic maar-diatreme volcanoes: a review". *Bulletin of Volcanology* 79.2. issn: 1432-0819. doi: 10.1007/s00445-016-1097-1.

Ross, P.-S., S. Delpit, M. J. Haller, K. Németh, and H. Corbella (2011). "Influence of the substrate on maar–diatreme volcanoes — An example of a mixed setting from the Pali Aike volcanic field, Argentina". *Journal of Volcanology and Geothermal Research* 201.1-4, pp. 253–271. issn: 0377-0273. doi: 10.1016/j.jvolgeores.2010.07.018.

Suter, M., O. Quintero, and C. A. Johnson (1992). "Active faults and state of stress in the central part of the Trans-Mexican Volcanic Belt, Mexico 1. The Venta de Bravo Fault". *Journal of Geophysical Research* 97.B8, p. 11983. issn: 0148-0227. doi: 10.1029/91jb00428.

Tibaldi, A. (1995). "Morphology of pyroclastic cones and tectonics". *Journal of Geophysical Research: Solid Earth* 100.B12, pp. 24521–24535. doi: 10.1029/95jb02250.

Tsutsumi, H. and J. S. Perez (2013). "Large-scale active fault map of the Philippine fault based on aerial photograph interpretation". *Active fault research* 2013.39, pp. 29–37. doi: 10.11462/afr.2013.39_29.

Turrin, B. D., J. T. Gutmann, and C. C. Swisher (2008). "A 13±3 ka age determination of a tholeiite, Pinacate volcanic field, Mexico, and improved methods for 40Ar/39Ar dating of young basaltic rocks". *Journal of Volcanology and Geothermal Research* 177.4, pp. 848–856. issn: 0377-0273. doi: 10.1016/j.jvolgeores.2008.01.049.

Valentine, G. A., J. D. L. White, P.-S. Ross, A. H. Graettinger, and I. Sonder (2017). "Updates to Concepts on Phreatomagmatic Maar-Diatremes and Their Pyroclastic Deposits". *Frontiers in Earth Science* 5. issn: 2296-6463. doi: 10.3389/feart.2017.00068.

van den Hove, J., L. Grose, P. G. Betts, L. Ailleres, J. Van Otterloo, and R. A. Cas (2017). "Spatial analysis of an intra-plate basaltic volcanic field in a compressional tectonic setting: South-eastern Australia". *Journal of Volcanology and Geothermal Research* 335, pp. 35–53. issn: 0377-0273. doi: 10.1016/j.jvolgeores.2017.02.001.

Vogel, T. A., T. P. Flood, L. C. Patino, M. S. Wilmot, R. P. R. Maximo, C. B. Arpa, C. A. Arcilla, and J. A. Stimac (2006). "Geochemistry of silicic magmas in the Macolod Corridor, SW Luzon, Philippines: evidence of distinct, mantle-derived, crustal sources for silicic magmas". *Contributions to Mineralogy and Petrology* 151.3, pp. 267–281. issn: 1432-0967. doi: 10.1007/s00410-005-0050-7.

Von Veh, M. W. and K. Németh (2009). "An assessment of the alignments of vents based on geostatistical analysis in the Auckland Volcanic Field, New Zealand". *Géomorphologie : relief, processus, environnement* 15.3, pp. 175–186. doi: 10.4000/geomorphologie.7664.

White, J. and P.-S. Ross (2011). "Maar-diatreme volcanoes: A review". *Journal of Volcanology and Geothermal Research* 201.1-4, pp. 1–29. issn: 0377-0273. doi: 10.1016/j.jvolgeores.2011.01.010.